29th EPS Conference on Plasma Phys. and Contr. Fusion Montreux, 17-21 June 2002 ECA Vol. **26B**, P-2.094 (2002)

Particle simulations of the magnetized hydrogen plasma-wall transition taking into account collisions with hydrogen atoms

D. Tskhakaya* and S. Kuhn

Association Euratom-ÖAW, Department of Theoretical Physics, University of Innsbruck, Innsbruck, Austria
**Permanent address: Institute of Physics, Georgian Academy of Sciences, Tbilisi, Georgia*

The plasma-wall transition (PWT), a narrow plasma region in front of a conducting wall, strongly affects the particle and heat fluxes to the wall [1], [2] and thus influences all plasma-wall interaction processes. Unfortunately, the extremely high complexity of the different processes going on in the PWT makes practically impossible quantitative analytic treatment. Even in numerical simulations, only simplified models of the PWT are used. Among these simplifications one usually finds the assumption of constant collision cross sections (or constant collision frequencies) for collisions between charged and neutral particles. In reality, however, these cross sections (or collision frequencies) strongly depend on the energy of the colliding particles and in general the related angular differential cross sections are strongly anisotropic.

In the present work we report the results of 1d3v (one spatial and three velocity dimensions) particle-in-cell (PIC) simulations of the magnetized hydrogen PWT and benchmark them with similar simulations of a simplified PWT model. In our present simulations we use a precise model for electron – atomic hydrogen and ionic hydrogen (proton) – atomic hydrogen collisions.

For the simulations we use the BIT1 code [3], developed on the basis of the XPDP1 code [4]. The following charged–neutral particle collisions are implemented via a Monte-Carlo subroutine [5]: electron - atomic hydrogen elastic ($e + H \rightarrow e + H$), excitation ($e+H \rightarrow e+H^*$), and impact ionization ($e+H \rightarrow 2e+H_+$) collisions, as well as ionic hydrogen - atomic hydrogen elastic ($H_+ + H \rightarrow H_+ + H$) and charge-exchange ($H_+ + H \rightarrow H + H_+$) collisions. Atomic hydrogen represents the fixed background with given density and temperature.

Electron impact ionization is described by the triply differential cross section [6]

$$\frac{d^3\sigma_{ion}}{dE_s d\Omega_p d\Omega_s} = \frac{d\sigma_{ion}}{dE_s}(E_p, E_s)\,\frac{d\sigma_{ion}}{d\Omega_p}(E_p, \cos\theta_p)\,\frac{d\sigma_{ion}}{d\Omega_s}(E_s, \cos\theta_s), \tag{1}$$

where E_p and E_s are the primary and secondary electron energies, and Ω_p and Ω_s are the solid scattering angles of the primary and secondary electrons, respectively; θ_p and θ_s are the corresponding scattering angles in the center-of-mass system; $d\sigma_{ion}/dE_s$, $d\sigma_{ion}/d\Omega_p$ and $d\sigma_{ion}/d\Omega_s$ represent the secondary electron energy and the primary and secondary electron angular distribution functions, respectively; $d\sigma_{ion}/dE_s$ and the corresponding integral cross section σ_{ion} are given as [6]

$$\begin{aligned}
\frac{d\sigma_{ion}}{dE_s} &= 5.511\times10^{-20}\frac{1}{E_{ion}\,(\varepsilon_p+1)}\left[\frac{1}{(\varepsilon_s+1)^2}+\frac{1}{(\varepsilon_p-\varepsilon_s)^2}-\frac{1}{\varepsilon_p+E_{ion}}\times\right.\\
&\left.\left(\frac{1}{\varepsilon_s+1}+\frac{1}{\varepsilon_p-\varepsilon_s}\right)+\ln\varepsilon_p\sum_{i=0}^{3}\frac{a_i}{(\varepsilon_s+1)^{3+i}}\right]\ m^2/eV\ , \qquad (2)\\
\sigma_{ion} &= \int_0^{(E_p-E_{ion})/2}\frac{d\sigma_{ion}}{dE_s}dE_s=\frac{5.511\times10^{-20}}{\varepsilon_p+1}\left[1-\frac{1}{\varepsilon_p}-\ln\varepsilon_p\sum_{i=0}^{5}\frac{b_i}{(\varepsilon_p+1)^i}\right]\ m^2,
\end{aligned}$$

where $\varepsilon_p = E_p/E_{ion}$, $\varepsilon_s = E_s/E_{ion}$, $E_{ion}(=13{,}606\ eV)$ is the ionization energy and

$$\begin{aligned}
a_0 &= -0.014353,\ a_1 = 0.75206,\ a_2 = -0.29548,\ a_3 = 0.056884\ ,\\
b_0 &= 0.18102,\ b_1 = -1,\ b_2 = 0.028706,\ b_3 = -2.0055,\ b_4 = 1.1819,\ b_5 = -0.36406\ ;
\end{aligned}$$

σ_{ion} as a function of primary electron energy is plotted in the Fig. 1(a).

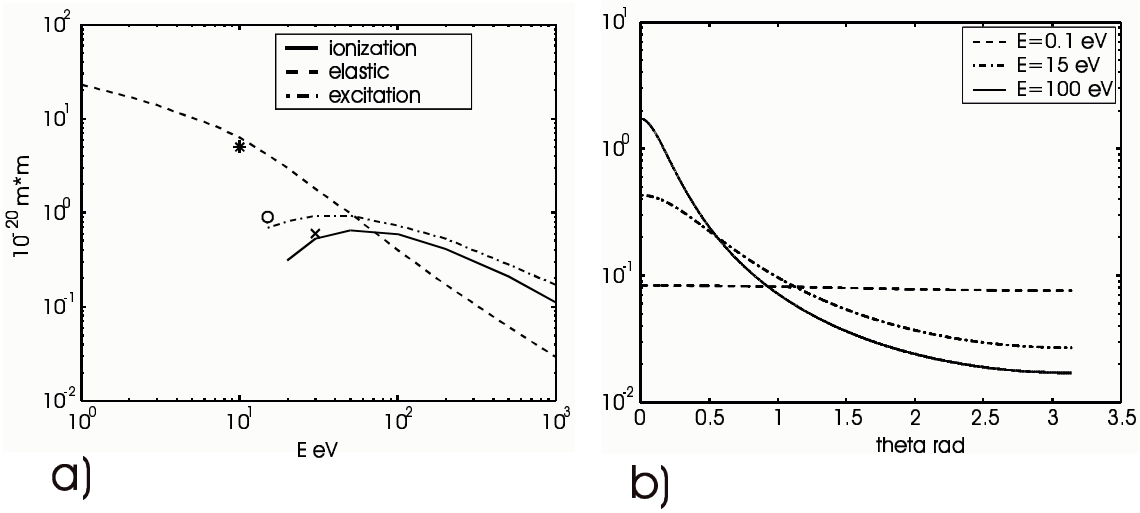

Figure 1: a) Electron-atomic hydrogen collision integral cross sections. $*$, o and $\times$ denote constant cross-sections for elastic, exitation and ionization collisions, respectively, which are used in the simplified model. b) Angular distribution of primary and secondary electrons.

For the angular distributions (of both primary and secondary electrons) we use the following empirical distribution function (see [5], [7] and [8]):

$$\frac{d\sigma_{ion}}{d\Omega} = \frac{1}{4\pi \ln(1+\alpha E)} \frac{\alpha E}{1+\alpha E \sin^2\theta/2}, \tag{5}$$

where $\alpha = 1$, $E = E_p - E_{ion}$, $\theta = \theta_p$ for primary and $E = E_s$, $\theta = \theta_s$ for secondary electrons. This distribution function has two advantages: (a) it takes into account an increasing anisotropy at high energies (see Fig. 1(b), and (b) it is relatively simple and allows an analytic expression for $\cos\theta$:

$$\cos\theta = \frac{1}{E}\left(2 + E - 2\,(1+E)^R\right), \tag{6}$$

where R is a random number ($R \in [0,1]$).

The integral cross sections of the elastic collisions, $\sigma_{el,e}(E)$, and the excitation collisions (total cross section: $1s- > 2s$, $2p$, $(2s+2p)$), $\sigma_{ex}(E)$, implemented in the code are plotted in Fig. 1 [6]. Here, E is the electron energy in the center-of-mass system. The angular distribution of the scattered electrons is given by (5).

The integral cross sections of the elastic collisions, $\sigma_{el,H}(E)$, and of the charge-exchange collisions, $\sigma_{cx}(E)$, between ionic and atomic hydrogen are given by [6]

$$\sigma_s(E) = c_0 \exp\left(\sum_{i=1}^{6} c_i (\ln E)^i\right) \times 10^{-18}\ m^2, \quad s = el, cx, \tag{8}$$

where E is the energy in the center-of-mass system and the coefficients c_i are given in Table 1.

For energies higher than $100\,eV$ we use an extrapolation (i.e., we use the same Eq. (8)) which is in excellent agreement with data from [9]. $\sigma_{el,H}(E)$ and $\sigma_{cx}(E)$ are plotted in Fig. 2(a).

The angular distribution for the elastic collisions in the center-of-mass system is described by Eq. (5). The best fit to the existing data [10] we obtained for $\alpha = 1.5 \times 10^5$ (see Fig. 2). The scattering angle in the laboratory system, χ, is calculated according to

$$\cos\chi = \sqrt{(1-\cos\theta)/2}\,. \tag{1}$$

Table 1

	elastic	collisions	charge exchange	collisions
	$0.001 \leq E \leq 10\ eV$	$E > 10\ eV$	$0.001 \leq E \leq 10\ eV$	$E > 10\ eV$
c_0	1.6050442	1.6184216	0.4526986	0.4605155
c_1	-0.1640510	-0.165075	-0.1000134	-0.1358551
c_2	$-4.995055e-3$	0	$-4.543425e-3$	0
c_3	$6.936219e-4$	0	$-3.587916e-3$	0
c_4	$1.423218e-3$	0	$-1.446320e-5$	0
c_5	$-1.622733e-4$	0	$9.322700e-5$	0
c_6	$-3.998204e-5$	0	$1.665865e-5$	0

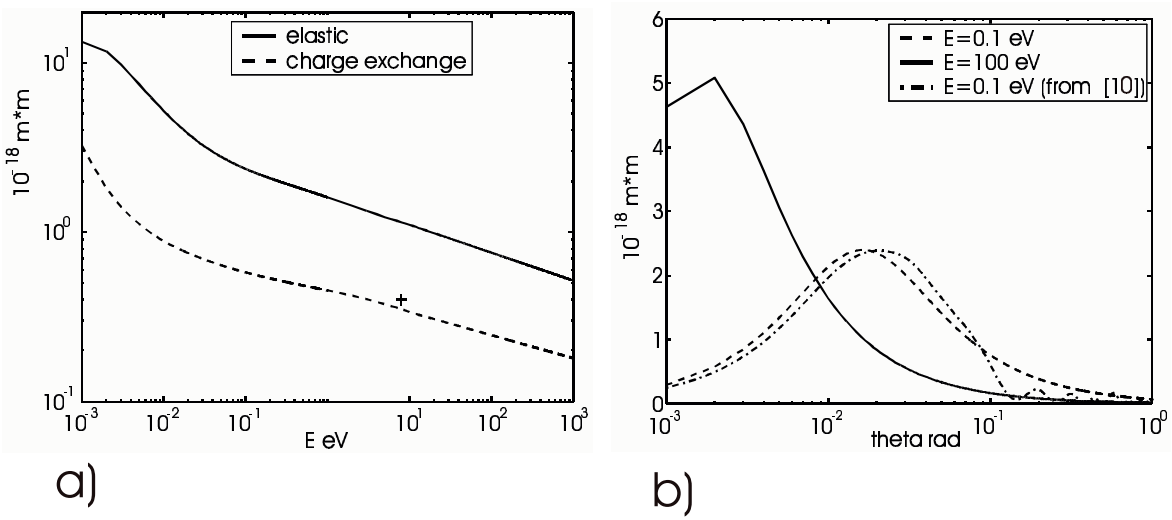

Figure 2: a) Ionic-atomic hydrogen collision integral cross sections. $*$ denotes the constant cross-section of the charge-exchange collision, which is used in the simplified model. b) Scattering angle distribution of the elastic collisions in the center-of-mass system.

Simulation geometry represents a one-dimensional magnetized plasma slab between two conducting walls. In the center of the system there is an ambipolar Maxwell-distributed particle (ion and electron) source. Particles reaching the wall are absorbed. In this model, all components of the PWT (the Debye sheath as well as the magnetic and collisional presheaths) develop self-consistently (for details of the simulation see [3]). The plasma parameters are chosen so as to be relevant to tokamak plasmas: the magnetic field strength, the inclination angle of the magnetic field to the wall, and the plasma density and temperature in the source region are $1\ T$, $5°$, $10^{18} m^{-3}$ and $T_{i,e} \sim 30\ eV$, respectively. During the simulation the ion and electron motions are fully resolved in space and time. The average number of simulation particles per spatial grid cell is about 300.

We ran two simulations: one with the precise model of the charged-neutral collisions and one with a simplified model of these collisions. For the simplified model we have used the usual assumption of constant cross-sections for all collisions and neglected elastic collisions between ionic and atomic hydrogen (see Figs. 1(a) and 2(a)). The angular distribution of the scattered electrons is given in the expression (5). The profiles obtained for the plasma parameters, averaged over a few hundred plasma oscillation periods, are shown in Fig. 3. The results are surprising in that there is no significant difference between the PWT with the accurate and the one with the simplified model of the charged-neutral collisions.

The main result of our simulations can be summarized as follows: For parameters relevant to high-temperature ($\geq 2\ eV$) fusion edge plasmas, the hydrogen PWT (and probably the deuterium and tritium PWTs as well) can be described with high accuracy

by a simplified PWT model. By "simplified PWT model" we mean one without elastic collisions between ionic and atomic hydrogen, and with constant cross-sections of other charged-neutral particle collisions.

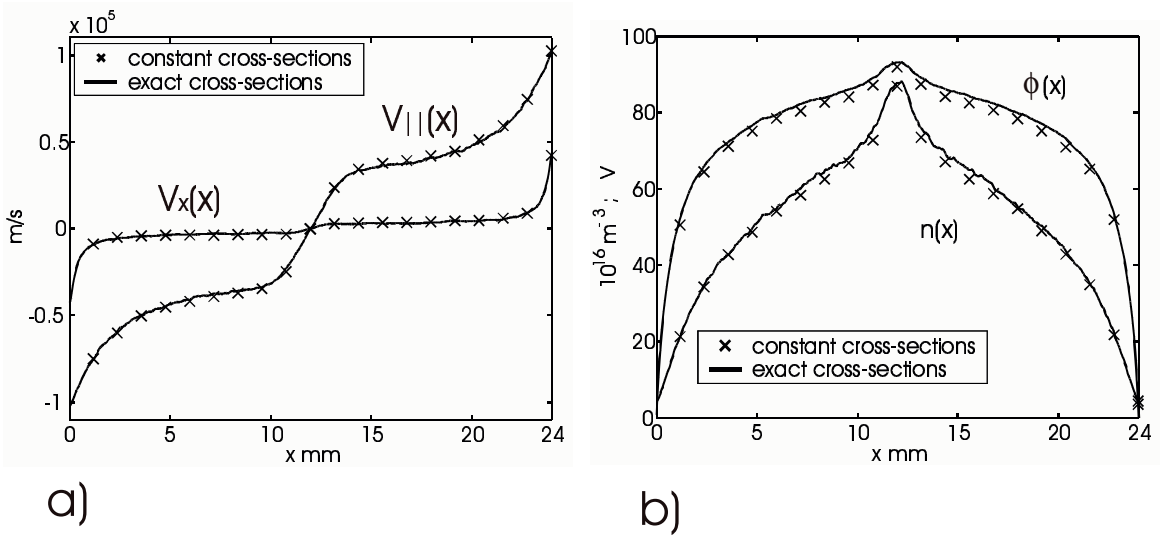

Figure 3: a) Profiles of the normal to the wall (V_x) and parallel to the magnetic field ($V_{||}$) components of the ion velocity. b) Profiles of the plasma potential (ϕ) and the ion density (n).

Acknowledgement. This work was supported by Austrian Science Fund (FWF) Project P15013 and has been carried out within the Association Euratom-ÖAW. Its content is the sole responsibility of the authors and does not necessarily represent the views of the Commission or its Services.

References

[1] P.C. Stangeby, The plasma boundary of magnetic fusion devices, IOP, Bristol and Philadelphia, 2000.
[2] K. -U. Riemann, Theory of the plasma-sheath transition, J. Tech. Phys. 41 (1), 89 (2000).
[3] D. Tskhakaya and S. Kuhn, Contrib. Plas. Phys., 42 (2-4), 302 (2002).
[4] J.P. Verboncoeur , M.V. Alves, V. Vahedi, and C.K. Birdsall, J. Comput. Phys. 104, 321 (1993).
[5] C.K. Birdsall, IEEE Transactions on Plasma Science, 19 (2), 65 (1991).
[6] R.K Janev (Ed.), Atomic and Molecular Processes in the Fusion Edge Plasmas, Plenum Press, New Yourk and London, (1995).
[7] M. Surendra, D.B. Graves, and G.M. Jellum, Phys. Rev. A, 41 (2), 1112 (1990).
[8] V. Vahedi, M. Surendra, Computer Phys. Comm., 87 179 (1995).
[9] Atomic Data for Fusion. Volume 1: Collisions of H, H2, He, and Li Atoms and Ions with Atoms and Molecules, C. F. Barnett ed., ORNL-6086 (1990).
[10] P.S. Krstić and D.R. Schultz, Atomic and plasma-material interraction data for fusion, Nucl. Fus. Suppl. 8 (1998).